


Pose-independent 3D Anthropometry from Sparse Data

David Bojanić^{1,2} , Stefanie Wuhrer² , Tomislav Petković¹ , and Tomislav Pribanić¹ 

¹ University of Zagreb Faculty of Electrical Engineering and Computing, Zagreb, Croatia

{david.bojanic, tomlav.petkovic.jr, tomlav.pribanic}@fer.unizg.hr

² Inria centre at the University Grenoble Alpes, Grenoble, France
{first.last}@inria.fr

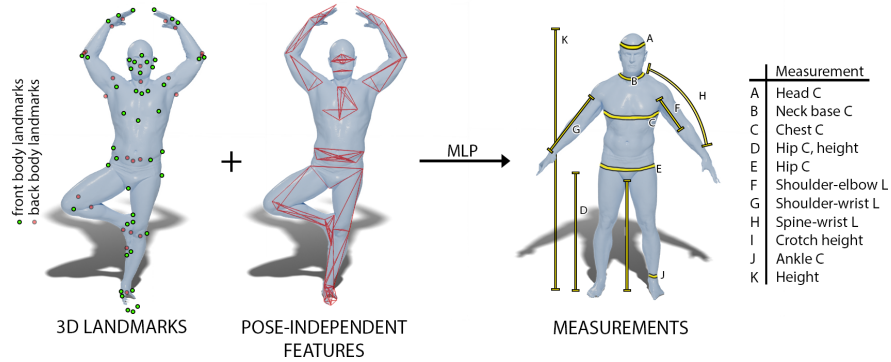


Fig. 1: We propose a new approach to estimate body measurements from 3D landmark locations on a body in any given pose. We identify pose-independent features that have an impact on the measurements by analyzing the landmarks of a large database of posed scans. The 11 body measurements listed on the right, are estimated from the 70 landmarks listed on the left, along with 158 pose-independent features in the middle.

Abstract. 3D digital anthropometry is the study of estimating human body measurements from 3D scans. Precise body measurements are important health indicators in the medical industry, and guiding factors in the fashion, ergonomic and entertainment industries. The measuring protocol consists of scanning the whole subject in the static A-pose, which is maintained without breathing or movement during the scanning process. However, the A-pose is not easy to maintain during the whole scanning process, which can last even up to a couple of minutes. This constraint affects the final quality of the scan, which in turn affects the accuracy of the estimated body measurements obtained from methods that rely on dense geometric data. Additionally, this constraint makes it impossible to develop a digital anthropometry method for subjects unable to assume the A-pose, such as those with injuries or disabilities. We propose a method that can obtain body measurements from sparse landmarks acquired in any pose. We make use of the sparse landmarks of the posed subject to create pose-independent features, and train a network to

predict the body measurements as taken from the standard A-pose. We show that our method achieves comparable results to competing methods that use dense geometry in the standard A-pose, but has the capability of estimating the body measurements from any pose using sparse landmarks only. Finally, we address the lack of open-source 3D anthropometry methods by making our method available to the research community at github.com/DavidBoja/pose-independent-anthropometry.

Keywords: 3D anthropometry · Body measurements · 3D body landmarks

1 Introduction

Anthropometry is the scientific study of measurements and proportions of the human body [5]. It encompasses the whole process from data collection, documentation, summarization, and analysis of body measurements [70]. These measurements are essential in quantifying the variations in populations and comparing populations of different countries, and ages [9, 49, 60], and it impacts a variety of industries, such as: medicine [15, 25], surveying [19, 70], fashion [70], fitness [10], and entertainment [12].

Manual anthropometry has been standardized [29] in order to achieve comparability between different subjects with different shapes. The procedure is carried out by an anthropometrist with the help of various tools, such as tape measures and calipers [70]. The standard protocol is comprised of several steps: (1) posing the subject in order to mitigate the influence of the pose onto the final measurement estimation; (2) finding the subject’s landmarks which are used as anchors to guide the measurement estimation and; (3) taking the measurement by using the appropriate tool to do so. As an example of taking the chest circumference, the subject is asked to stand upright and exhale, while the tape measure is wrapped around the torso passing through the left and right Thelion landmarks [29]. The manual anthropometry standards are the main constraint for efficient and widely available anthropometry since anthropometrists need to be trained in order to estimate accurate measurements [21, 43], and obtaining the measurements takes significant time [5].

With digital anthropometry, the expert anthropometrists are replaced with digital devices, such as 3D scanners, mobile phones and various sensors. The standards, however, remain [28], but are mostly shifted onto the subject being measured instead of the one doing the measuring. These standards are related to the 3D scanning process and are the main constraints of 3D digital anthropometry. In order to scan a subject for measurement estimation, they need to stand in the fixed A-pose (upright standing pose with feet and hands slightly apart) without moving during the scanning, which can last up to 5 minutes with handheld scanning devices [5].

This is a great obstacle to having an efficient and more accessible anthropometry method, as even the subject’s breathing can affect the precision of the final measurements [5, 58]. Since most methods require dense geometric data in order

to estimate the measurements, this hinders their performance. Furthermore, requiring the fixed A-pose in order to estimate the body measurements excludes the subjects with injuries and disabilities [52, 54] or those prone to fidgeting [5].

Most of the methods that estimate body measurements of posed subjects, do not generalize well to poses diverging from the standard A-pose [48, 50], can only generalize to the sitting pose [57] or purposefully diverge from the A-pose measurements to model the change in shape of a dynamic sequence [59].

To alleviate these constraints, we propose a simple method that can estimate the body measurements from sparse landmarks in any pose. To do so, we identify features that are pose-independent and have an impact on the measurements, by analyzing a large database of posed scans. Using the landmark coordinates and the identified features we estimate the measurements as in the standard A-pose. The 3D body landmark coordinates can be estimated from posed body scans using existing approaches, such as [39, 65, 67]. In this work we assume the landmarks are given and focus on estimating the measurements. This assumption is in line with the current literature, since most of the methods assume landmarks either for template fitting [34, 44, 57, 59, 63, 68], measurement estimation [1, 13, 23, 36, 38, 42, 50, 56, 61, 67, 71], or use other similar priors [16, 64].

A great challenge with the 3D anthropometry literature are the limited number of open-source datasets and virtually no open-source implementations. Most works create a private small-scale dataset [17, 30, 31, 34, 38, 42, 48, 56, 61, 63, 64, 67, 71] in order to test their method on several human body scans, and do not share it with the community due to privacy issues. Furthermore, to the best of our knowledge, none of the works, except [7], share their code implementations with the community, making the comparison between different methods impossible. We compare our method with [3, 7, 24, 57] which share their results on the commercial CAESAR [49] dataset, and with [48] on the DYNA [46] dataset. To make a step towards a more open source 3D anthropometry research, we share the exact subjects and scans we evaluate our method on, and make our implementation available at github.com/DavidBoja/pose-independent-anthropometry.

In summary, our contributions are:

- A method to estimate body measurements in any given pose using only sparse landmark data.
- Making the method and detailed evaluation protocol available to the research community.

2 Related work

We first give a general overview of related works that estimate body measurements, after which we focus on methods that estimate the measurements from posed subjects.

2.1 3D anthropometry

Existing approaches for automatic body measurement estimation from 3D scans fall into three categories: landmark-based, template-based, and direct methods.

Landmark-based methods use 3D landmarks and dense scan data to estimate the measurements [1, 13, 23, 36, 38, 42, 50, 56, 61, 67, 71]. Length measurements can be estimated as Euclidean or geodesic distances between the landmarks, and circumference measurements can be estimated by cutting the dense scan with a plane at a desired landmark location and finding the cross-section. Rather than cutting the scan with a plane, a path can also be found [66] or a curve can be fitted [1, 38, 56] to a set of landmarks from the body mesh. These methods, however, usually require prior information, such as the subject’s sex [38], orientation [36, 38, 42, 61], height [56], or pose [13, 50, 71]. Furthermore, these methods require dense scan data since they estimate the measurements directly from the given scan, which makes them sensitive to noise and missing data [31].

Our method, on the other hand, does not require any prior information, and estimates the measurements using only the landmark locations, therefore avoiding the necessity for dense scan data. Furthermore, by learning the measurements, we can address the method’s sensitivity to noise in the data.

Template-based methods fit a template to a 3D scan from which the measurement can be learned, transferred, or estimated from 3D landmarks. To learn the measurements [24, 34, 44, 57, 64, 68] extract a combination of features from the fitted template (such as the 3D points, predefined paths, shape parameters, mesh edge lengths, or PCA coefficients of triangle deformations) to train different models, such as the ElasticNet [72], SVR [11] and PLS [18]. To transfer the measurements [16, 30, 31, 59, 63] predefine the body measurement paths on the template, which can (optionally) be transferred onto the scan by finding the nearest neighbor of each path point from the template to the scan. Similarly, to estimate the measurements from landmarks, [14, 17, 20, 62] transfer the landmarks from the template to the scan, and find the measurement using the landmark-based methods described above. Template-based methods tend to be sensitive to the fitting process [45], and are usually stabilized with additional information such as landmarks [68], texture maps [6, 46] or rendered silhouettes [64]. Additionally, similarly to landmark-based methods, template-based methods need dense scan data to accurately represent the shape of the subject.

In contrast, our method avoids the fitting process and does not need dense scan data to estimate the measurements.

Direct methods learn body measurements from the 3D scans. Whereas [3, 55, 73] learn to predict the measurements from the 3D points, [48] uses gradient-boosted trees to predict local measurements, which are weighted in order to compute the final measurements. A more recent method [7], uses the landmark locations to learn a Bayesian regression model that predicts the measurements. These methods resort to training their methods using synthetic datasets created with statistical human body models [37, 45]. Because of this, they tend to have difficulties in generalizing to real data.

Compared to direct methods, we train our method by posing 3D human scans with manual ground truth measurement annotations. Additionally, we only use the landmark coordinates as inputs to our method instead of the full scans.

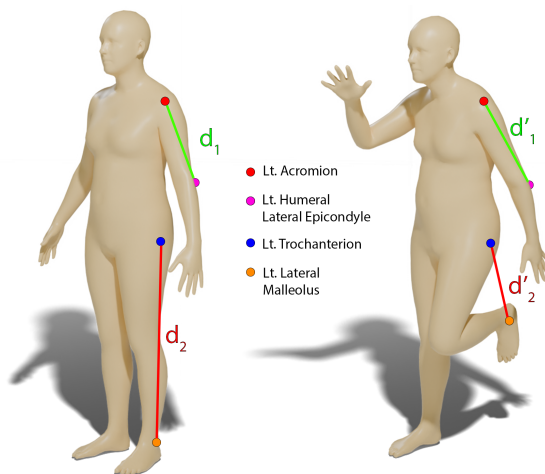


Fig. 2: We show the landmark distances of the same subject in two different poses. As can be seen, the same landmark distances d_1 and d'_1 do not significantly change between the two poses, observing an absolute difference of only 0.78 cm. On the contrary, the landmark distances d_2 and d'_2 change significantly because of the articulated deformation of the leg. In this case, the absolute difference between d_2 and d'_2 is 36.75 cm. In our method we only use landmark distances where the median difference from its appropriate A-pose distance is less than 1 cm, such as the distance d_1 .

This way, we minimize the synthetic-to-real domain gap by utilizing a simpler representation, which can be bridged more easily during training [51].

2.2 3D anthropometry from posed subjects

Some works estimate anthropometric measurements from poses that differ substantially from the standardized A-pose. Among landmark-based methods, Robinson and Parkinson [50] estimate only a few length measurements from joint locations predicted from a Microsoft Kinect [53]. Among template-based methods, Uriel et al. [59] extract the measurements directly from the fitted SMPL [37] body model to a sequence of motion, whereas Tsoli et al. [57] learn an Elastic-Net [72] model from a set of features extracted from the body model in two poses. Among direct methods, Probst et al. [48] use gradient-boosted trees to find the measurements from a depth map of the subject, whereas Yin and Zhou [69] use a CNN to learn the height of the subject.

Compared to these, our method can estimate multiple body measurements, avoids the template fitting process, does not rely on dense scan data, and generalizes well to different datasets. We compare our approach with approaches from different categories [3, 7, 24, 48, 57] that provide their results on the CAESAR and DYNA datasets.

3 Method

We learn a Multilayer Perceptron (MLP) to predict the 11 body measurements visualized in Fig. 1 (right). The inputs to our method are the 70 landmarks visualized in Fig. 1 (left). We normalize the landmark coordinates using the pelvis landmarks as follows: in the first step, we find the middle point between the Lt. and Rt. Psis landmarks, which we denominate as Middle Psis. Using this point, along with the Lt. and Rt. Asis landmarks, we create a triangle. The center of the triangle is then translated to the origin, whereas the triangle normal is aligned with the y -axis. The normal orientation is pointing towards the half plane containing the Nuchale landmark. Finally, we rotate the landmarks around the y -axis to align the Rt. Asis landmark with the z -axis. We unravel the normalized coordinates into a $70 \times 3 = 210$ dimensional vector to input into the model.

To facilitate learning, we additionally identify pose-independent features and provide them to the model. Intuitively, the distances between landmarks located on the same bone of the body should remain constant with pose variation. We show an example of the landmark features in Fig. 2, where the distance between the *Lt. Acromion* (shoulder landmark) and *Lt. Humeral Lateral Epicondyle* (elbow landmark) does not change with pose variation. Contrarily, the distance between the *Lt. Trochanterion* (hip landmark) and the *Lt. Lateral Malleolus* (foot landmark) changes a lot with pose variation since the body deforms in a non-rigid manner. To find the pose-independent landmark distances (features), we pose a single subject in around 410 000 poses, and analyze the differences of the corresponding landmark distances from their reference distance in the A-pose. Details about the posing are provided in Sec. 4.1. Finally, we choose the landmark distances that have a median difference less than 1 cm, which results in 158 landmark distances. Interestingly, as can be seen from the full set of pose-independent features in Fig. 1, the chosen features are not necessarily symmetric w.r.t. the body, since some of the features from the left (or right) side of the body have been selected, but their respective right (or left) counterparts have not. This happens for the landmark distances that are very close to the cutoff threshold of 1 cm, where one of the distances is slightly below the threshold, and its counterpart is slightly above. The difference between these counterparts is around 2 mm.

The final inputs to our model are comprised of 210 landmark coordinates and 158 landmark distances, resulting in a 368 dimensional input vector. We train our model using a MLP network with three layers of dimensions 194, 97 and 11 with a ReLu activation after the first two layers. We optimize the Mean Squared Error (MSE) between the predicted and ground truth 11 measurements.

4 Datasets

We train and evaluate our method on parts of the CAESAR [49] dataset, and evaluate it on parts of the DYNA [46] and 4DHumanOutfit [4] datasets. We specify the details of each dataset in the following.

4.1 CAESAR

The CAESAR dataset contains 4396 subjects scanned in the standing A-pose and two sitting poses. 73 body landmarks were manually annotated, from which we use the subset of 70 landmarks visualized in Fig. 1 (left). The subjects were manually measured, and we use a subset of 11 measurements shown in Fig. 1 (right) following common practice [57]. To compare with existing methods, we use the training / test split by Tsoli *et al.* [57] containing 1644 subjects (849 male, 795 female) for training and 400 subjects (200 male, 200 female) for testing. Of the training and testing subjects, 120 and 30 have at least one missing measurement or landmark, respectively. Therefore, we use the remaining 1424+100 subjects to train and validate, and the remaining 370 subjects to test our method. Depending on the pose, we train and evaluate on several different subsets of CAESAR, which we explain in the following.

Posed training set. To train our method on arbitrary poses, we augment the CAESAR dataset by reposing the 1424 training subjects into 12000 different poses. We start by fitting the SMPL model to the A-pose scans. We use a 2-step optimization technique [8]. In the first step, we optimize for the pose, shape, scale and translation parameters of the body model, which we supervise using the provided body landmarks. In the second step, we optimize for the SMPL template vertex locations. After fitting, the mean directional chamfer distance from the fitted template to the scans is 0.31cm, whereas the mean directional chamfer distance from the scans to the fitted templates is 1cm. We then use the fitted SMPL to unpose and repose the scans into a set of 12000 poses, comprised of 1000 standing poses, 1000 sitting poses and 10000 varying SMPL poses obtained from several datasets [27,33,40,41]. For each pose, we randomly choose a subject from the CAESAR training subjects, and repose them. Therefore, we train our method using the reposed landmarks and supervise it using the provided manual measurements.

Standing test set. We test our method on the standard A-pose provided by the CAESAR dataset. We evaluate on the 370 testing subjects and use the provided landmark coordinates and manual measurements.

Noisy test set. To observe the robustness of our method to landmarking errors, we augment the standing test set described above by moving the landmarks along the mesh up to 0.56cm, which corresponds to the average median manual inter-observer landmarking error for all the landmarks [32]. Each landmark is augmented by moving it along the cross-section of the scan and random plane obtained at the landmark point.

Sitting test set. The CAESAR dataset provides scans and landmarks for 4345 out of the 4396 subjects in the sitting B-pose. From these, no subject has all of



Fig. 3: Some of the poses used to create the posed test set. We augment the CAESAR dataset by reposing the subjects in various poses obtained from the AIST [35] dataset.

the landmarks necessary to test our method. Therefore, we transfer the missing landmarks from the fitted SMPL template. We evaluate on the same 370 testing subjects and use the provided manual measurements from the CAESAR dataset.

Posed test set. To test the pose-independency of our method, we use the same approach as for the training dataset to pose the testing subjects in various poses. We use a sample of 370 poses from the AIST [35] dataset, which is comprised of highly diverse poses obtained from real dancing subjects. Note that these poses have not been seen by the model during training. We visualize some of the poses in Fig. 3.

4.2 Dynamic test set

To test the robustness of our method w.r.t. motion, we follow [48] and estimate the measurements of a single subject during a jumping-jacks sequence from the DYNA [46] dataset (with id 50009). To obtain the landmarks, DYNA provides accurate SMPL fittings, from which we extract the 70 body landmarks. Since the ground truth measurements are not provided, we follow [48] and evaluate the standard deviation of the measurement difference between each frame and the first frame.

4.3 Clothed test set

To test the robustness of our method w.r.t. clothed subjects, we use a sample of the 4DHumanOutfit [4] dataset originally comprised of 18 subjects performing 10 actions in 6 different outfits. We use a subset of 6 subjects (namely Ben, Leo, Mat, Kim, Mia, and Sue) performing 3 actions (namely dance, run, avoid) in tight clothing, amounting to 5640 frames. Similarly to the DYNA evaluation, for each sequence we compute the difference between the first frame measurement estimation and the remaining ones. Then, we compute the standard deviation over these measurement differences for each measurement separately.

5 Experiments

We compare our method with three template-based methods [24,47,57] and three direct methods [3,7,48]. Among the template-based methods, [24,47] estimate

the measurements from the fitted template vertices, whereas Tsoli et al. [57] extract features from the fitted template in order to estimate the measurements. Among the direct methods, the commercial solution Anthroscan [3] estimates the measurements directly from the 3D points whereas Probst et al. [48] estimate them from a depth map of the subject using gradient-boosted trees.

All of the previously mentioned methods use dense scan data in order to estimate the measurements, and we report their results based on the training and test sets provided by [57]. For the methods operating on sparse landmark data, all tests are effected on the 370 scans for which all measurements and landmarks in the A-pose are available. The work from Bojanić et al. [7] is the only method that uses sparse landmarks in the A-pose to estimate the measurements. However, their approach is not adept to estimate the measurements in any other pose. To mitigate this and have a method to compare with in the *sparse data* category, we introduce a template-based baseline that can estimate the measurements from sparse data in any given pose. The baseline fits an SMPL body model to the given posed landmark coordinates. Next the SMPL is reposed to the A-pose by retaining the fitted shape, and measurements are extracted using the standard landmark-based approach, where distances between landmarks, as well as circumferences of cross-sections are measured, as described above. The baseline provides an insight into the difficulty of the problem, which stems from the ambiguity of using sparse landmark locations to estimate the measurements.

To further explore this ambiguity, we aim to answer the question whether different body shapes, with different measurements, can share the same landmarks. We use the SMPL model in the fixed neutral pose θ_0 to model the relationship between the landmarks and measurements. We start from a reference shape β_{ref} obtained by fitting the SMPL model to an arbitrary real subject from the CAESAR dataset. We manually mark the 70 SMPL landmarks as $L(\theta_0, \beta_{\text{ref}})$, whose locations depend on the same SMPL pose and shape parameters θ and β . We optimize for a displaced shape $\beta_{\text{ref}} + \delta$, that is at unit distant from the reference shape and has the closest landmarks in terms of the Euclidean distance to the reference landmarks. Then, by moving in the direction of the *optimized shape* $\beta_{\text{ref}} + k\delta$ for various steps k , we can observe the variation of the body measurements with almost no landmark variation. More precisely, we optimize:

$$\min_{\delta} \left(\sum_i \underbrace{\|L_i(\theta_0, \beta_{\text{ref}}) - L_i(\theta_0, \beta_{\text{ref}} + \delta)\|_2}_{\text{reference landmarks}} + \underbrace{\|\delta\|_2 - 1}_{\text{unit norm}} \right), \quad (1)$$

where L_i indicates the i -th landmark. Fig. 4 visualizes for each displacement k the maximum landmark distance between the reference and optimized shapes on the x -axis and the corresponding measurement error on the y -axis.

As can be seen, the relative change in body measurements is not proportional to the relative change in landmark displacement. When the maximum landmark distance between the reference and optimized shape reaches 1cm, the chest circumference, for example, reaches a high 2.7cm of change. This shows that estimating the body measurements from sparse landmark data is a diffi-

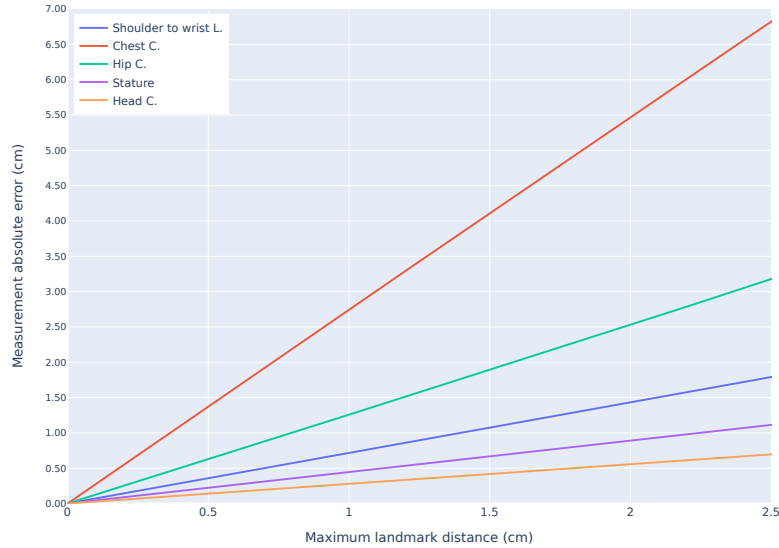


Fig. 4: We answer the question whether different body shapes, with different measurements, can share the same landmarks. The relationship between the landmarks and measurements is linear since it is modeled with SMPL, and shows an approximation of the relationship that would be obtained with real data. As can be seen, the chest and hip circumference measurements change faster than the landmark distances, indicating that two subjects can have close-by landmark coordinates with different chest and hip circumferences.

cult task since the measurements can be ambiguous for very similar landmark locations. Furthermore, the x -axis shows the maximum landmark distance up to 2.5cm, which is an average displacement of vertices that can be caused just by the subject’s breathing [58]. For that level of landmark distance, the chest measurement error goes up to 6.8cm.

To provide more context to the results obtained by the sparse methods, we show the ambiguity error for each measurement in the following evaluation tables for a fixed maximum landmark distance of 5.64mm, obtained as the average median landmarking manual error [32]. As is standard practice, we also add the allowable error (AE) [22] for manual measurements to the tables.

5.1 Metrics

For the static datasets where the ground truth manual measurements are provided, we use the mean absolute error (MAE) metric to evaluate our results. The MAE for a single measurement j is computed as:

$$MAE^j = \frac{1}{N} \sum_{i=1}^N |gt_i^j - est_i^j|, \quad (2)$$

Table 1: MAE in mm on the standing and noisy test sets (male subjects). The left shows results on the standing test set, whereas the right shows results on the noisy test set. We abbreviate the measurements as: Circumferences (C.), Heights (H.) and Lengths (L.).

Measurement	ORIGINAL DATA						AE [22]	Ambiguity	NOISY DATA		
	dense methods			sparse methods					sparse methods		
	[3]	[24]	[57]	baseline	[7]	Ours			baseline	[7]	Ours
Ankle C.	13.66	5.72	5.56	26.50	10.33	6.66	4	2.62	25.74	10.48	6.96
Shoulder-elbow L.	13.99	12.66	13.32	48.94	7.25	12.70	6	1.28	49.61	7.61	12.71
Shoulder-wrist L.	14.49	13.76	12.66	80.35	14.22	15.32	-	4.04	81.28	14.66	16.30
Spine-wrist L.	14.71	11.81	10.40	73.43	12.85	16.18	-	3.17	74.39	12.80	17.13
Chest C.	13.96	15.21	13.02	62.15	99.94	21.89	15	15.52	64.38	100.46	22.19
Crotch H.	11.01	9.77	8.36	13.04	26.73	8.80	10	2.37	12.96	31.09	12.50
Head C.	5.51	7.46	5.59	20.85	9.34	10.40	5	1.56	20.46	9.63	10.71
Hip C. H.	16.50	18.89	19.05	27.32	37.80	20.76	-	1.49	27.60	38.69	21.89
Hip C.	7.90	12.57	10.66	41.15	35.55	20.67	12	7.08	41.99	36.64	21.05
Neck base C.	21.57	13.33	13.47	65.26	14.33	16.99	11	1.67	63.03	14.66	16.81
Stature	5.86	7.98	6.53	13.90	25.09	11.68	10	2.52	14.08	25.46	11.85
aMAE	12.65	11.74	10.78	42.99	26.68	14.73			43.23	27.47	15.46

Table 2: MAE in mm on the standing and noisy test sets (female subjects). The left shows results on the standing test set, whereas the right shows results on the noisy test set. We abbreviate the measurements as: Circumferences (C.), Heights (H.) and Lengths (L.).

Measurement	ORIGINAL DATA						AE [22]	Ambiguity	NOISY DATA		
	dense methods			sparse methods					sparse methods		
	[3]	[24]	[57]	baseline	[7]	Ours			baseline	[7]	Ours
Ankle C.	7.55	6.59	6.19	15.77	16.69	7.01	4	2.62	15.50	16.42	7.04
Shoulder-elbow L.	11.26	8.42	6.65	29.89	6.19	7.27	6	1.28	29.92	5.91	7.24
Shoulder-wrist L.	11.67	10.42	10.05	57.29	22.24	9.11	-	4.04	57.26	22.77	9.73
Spine-wrist L.	13.19	13.40	11.87	57.04	12.94	12.70	-	3.17	56.77	13.42	13.51
Chest C.	12.43	13.02	12.73	33.28	37.67	20.54	15	15.52	33.99	37.03	20.66
Crotch H.	7.45	7.53	5.50	10.70	50.49	6.93	10	2.37	10.69	39.79	14.07
Head C.	7.44	7.45	5.91	18.59	9.11	9.70	5	1.56	18.41	9.20	9.62
Hip C. H.	17.05	18.96	18.59	32.70	36.38	20.00	-	1.49	32.65	36.20	20.24
Hip C.	7.47	16.15	12.35	38.48	25.61	22.61	12	7.08	39.00	24.29	22.60
Neck base C.	21.03	16.35	15.43	73.53	17.19	17.10	11	1.67	72.75	17.69	17.31
Stature	5.60	10.21	7.51	13.35	36.85	9.79	10	2.52	14.38	36.74	10.03
aMAE	11.10	11.68	10.25	34.60	24.67	12.98			34.67	23.59	13.82

where N is the number of subjects, gt_i^j is the ground truth measurement for subject i and measurement j and est_i^j is the estimate of measurement j for subject i . We further provide the average mean absolute error (aMAE) which averages the MAEs over the 11 measurements for each method.

For the dynamic and clothed test sets, where the ground truth measurements are not provided, we follow [48] and use the standard deviation over the difference between the measurements of each frame and the first frame.

5.2 Standing pose

We compare our results on the CAESAR test subjects in the standard standing A-pose. We show the results for the male and female subjects separately in Tables

1 and 2. Comparing the two tables, we can notice that the errors for the female subjects are in general lower for all the methods. The results indicate that the arm lengths for the male subjects are harder to estimate.

We first analyze results of methods that use dense scan data as input. Anthroscan [3], achieves the lowest MAE for the hip circumference. Anthroscan extracts the measurements directly from the dense scan data, without using a body template or relying on accurate landmark data. However, the method achieves the worst average results among methods that rely on dense data. The template-based method [24] performs slightly better (on average) than Anthroscan by fitting the SCAPE [2] body model onto the scan, and using a linear model to predict the measurements from the template vertices. Tsoli et al. [57] improve on this by fitting a BlendSCAPE [26] body model to the 3D scan and extracting complex features from the template to learn the measurement. By using more sophisticated features, such as a set of predefined paths, PCA coefficients of the body model fitting, and limb lengths, they achieve the best results because they considers a much greater number of local and global features.

Second, we consider works that only use sparse landmark locations as input, which avoids the requirement of dense data and template fitting. Among sparse methods, our approach achieves the best results followed by [7] and the baseline, respectively. The main limitation of our approach are the chest and hip circumferences which have an error over 20 mm. However, as we see from the ambiguity column and Fig. 4, these measurements have the largest ambiguity in terms of landmark locations. Note that our approach achieves results that are only 3.34 mm less accurate on average than the best method operating on dense data.

When testing on the noisy test set (right of Tab. 1 and 2), it is interesting to note that all the sparse methods, including ours, are robust to noise, and achieve only slightly worse results when landmarking errors are introduced.

5.3 Sitting pose

We compare results on the sitting test set in Tab. 3. The errors increase w.r.t. the standard A-pose. The main challenge with the sitting pose is the occlusion of the back of the body due to the pose. This affects the template-based methods [24,57] and the baseline, since the fitting relies on dense scan data. Among the sparse methods, [7] has only been trained on the A-pose, and is therefore not adept to estimating the measurements from posed landmarks. Our approach outperforms other sparse methods by a large margin and is only about *5mm* less accurate on average than for the standing test set. The main reason to the degradation are the missing landmarks, as all scans in this test set suffer from missing landmarks. The landmarks are therefore transferred from the SMPL fitting for our approach and [7], and additionally reposed for the baseline. Compared to the best dense method, our method is only 6.44 mm less accurate on average.

Table 3: MAE in mm on the sitting test set. We abbreviate the measurements as: Circumferences (C.), Heights (H.) and Lengths (L.). Ambig. stands for ambiguity.

Measurement	MALE						FEMALE						AE [22]	Ambig.
	dense		sparse			dense		sparse						
	[24]	[57]	baseline	[7]	Ours	[24]	[57]	baseline	[7]	Ours				
Ankle C.	5.79	5.22	29.97	11.81	7.05	7.00	6.36	19.03	31.64	7.57	4	2.62		
Shoulder-elbow L.	13.83	13.07	47.34	57.80	12.05	8.09	6.66	26.83	50.04	9.91	6	1.28		
Shoulder-wrist L.	12.75	12.29	79.14	122.21	15.21	10.89	10.49	54.77	151.11	10.56	-	4.04		
Spine-wrist L.	11.61	11.26	67.39	115.07	18.37	13.16	12.34	52.45	164.30	12.72	-	3.17		
Chest C.	15.40	13.86	95.77	49.69	26.63	13.48	13.05	84.59	129.33	21.57	15	15.52		
Crotch H.	14.19	14.54	29.85	149.51	19.87	11.03	9.66	16.59	131.48	17.13	10	2.37		
Head C.	6.51	5.42	17.71	28.98	9.76	7.45	5.67	17.43	28.91	10.35	5	1.56		
Hip C. H.	21.41	20.84	42.27	179.59	25.17	23.72	22.26	29.73	147.54	27.07	-	1.49		
Hip C.	13.84	13.68	62.17	36.87	30.33	17.34	15.48	48.30	61.30	58.47	12	7.08		
Neck base C.	13.33	13.47	52.60	18.79	14.79	16.96	15.79	52.49	24.19	17.96	11	1.67		
Stature	10.59	8.99	18.28	328.21	15.93	11.40	10.28	16.30	284.39	13.80	10	2.52		
aMAE	12.65	12.05	49.32	99.86	17.74	12.77	11.64	38.05	109.48	18.83				

Table 4: MAE in mm on the posed test set. We abbreviate the measurements as: Circumferences (C.), Heights (H.) and Lengths (L.).

Measurement	MALE			FEMALE			AE [22]	Ambiguity
	Baseline	[7]	Ours	Baseline	[7]	Ours		
Ankle C.	25.92	23.13	6.62	18.25	20.00	7.29	4	2.62
Shoulder-elbow L.	47.45	76.02	14.86	35.79	64.07	8.47	6	1.28
Shoulder-wrist L.	78.06	210.35	17.18	66.33	187.68	11.10	-	4.04
Spine-wrist L.	62.81	210.21	19.35	71.36	191.05	15.89	-	3.17
Chest C.	74.27	120.77	29.17	26.38	109.69	26.18	15	15.52
Crotch H.	13.23	34.34	10.61	11.27	40.20	8.13	10	2.37
Head C.	20.45	32.56	10.44	22.21	39.16	10.61	5	1.56
Hip C. H.	28.28	72.53	22.99	32.59	60.61	20.68	-	1.49
Hip C.	41.10	92.59	20.91	40.66	62.73	25.39	12	7.08
Neck base C.	63.33	48.21	17.39	82.48	41.42	17.08	11	1.67
Stature	17.19	74.62	14.62	13.70	57.25	13.99	10	2.52
aMAE	42.92	90.49	16.74	38.27	79.44	14.98		

5.4 Arbitrary pose

In this section we analyze the pose-independence of our approach. We evaluate our method on the posed, dynamic and clothed test sets.

Semi-synthetic data. We evaluate our approach on the posed test set in Tab. 4. As can be seen, both the baseline and [7] do not have the capability to estimate the measurements from posed subjects. Contrarily, our approach achieves very similar results to the standard A-pose. This shows that our approach is robust to pose changes as long as reliable landmark input is provided (unlike in the case of the sitting pose, where landmark information was missing).

Scan data. We evaluate our approach on the dynamic test set in Tab. 5 and the clothed test set in Tab. 6. We compute the standard deviation of the difference between each frame and the first frame. This way we can analyze the

Table 5: Standard deviation in cm of the estimated sequence measurements for the dynamic test set.

Measurement	[47]+ICP	[48]	Ours
Arm L.	1.16	0.77	0.43
Hip C.	1.78	1.70	0.65

Table 6: The standard deviation in mm on the clothed test set.

Measurement	Std (mm)	Measurements	Std (mm)
Ankle C.	2.05	Head C.	4.19
Shoulder to elbow L.	2.58	Hip C. H.	8.45
Shoulder to wrist L.	3.34	Hip C.	7.51
Spine to wrist L.	4.34	Neck base C.	3.90
Chest C.	12.51	Stature	11.29
Crotch H.	8.11		

consistency of our approach w.r.t. a dynamic change in pose, or even change in pose obstructed by clothing. As we can see from both tables, our approach behaves consistently with slight variations to the measurements during the dynamic movement. This indicates that even though our approach has an error of around 15 mm for a subject on average (seen in previous results), it consistently predicts the same measurements for a single subject, achieving pose-independence. For the dynamic test set, Tab. 5 further shows that our approach slightly outperforms the state-of-the-art dynamic method on the two measurements for which results are available.

6 Conclusion

The current pipeline for 3D anthropometry consists of scanning the subject in the static A-pose without any movement. However, the A-pose is not easy to maintain during a scanning process that can last up to a couple of minutes. This constraint affects current state-of-the-art template-based methods that rely on dense geometry data. Additionally, this constraint makes it impossible to develop a digital anthropometry method for subjects unable to assume the A-pose, such as those with injuries or disabilities. We propose a robust approach that estimates body measurements from any given pose using only sparse landmark data. We thoroughly test our method and show that it achieves comparable results to the state-of-the-art methods operating on dense scan data in the standard A-pose, but has the capability of estimating the body measurements from landmark data only, acquired in any pose. We address the lack of open-source 3D anthropometry methods by making our method available to the research community.

Acknowledgement

This work has been supported by the Croatian Science Foundation under the projects IP-2018-01-8118 and DOK-2020-01, as well as the European Union - NextGenerationEU. Views and opinions expressed are however those of the author(s) only and do not necessarily reflect those of the European Union or European Commission. Neither the European Union nor the European Commission can be held responsible for them. We thank Antoine Dumoulin and Rim Rekik Dit Nkhili for helping with the SMPL fitting and Briac Toussaint for helping with the visualizations. In memory of our dear colleague and friend, Tomislav Pribanić.

References

1. Albances, X., Binungcal, D., Nikko Cabula, J., Cajayon, C., Cabatuan, M.: Rgb-d camera based anthropometric measuring system for barong tagalog tailoring. In: 2019 IEEE 11th International Conference on Humanoid, Nanotechnology, Information Technology, Communication and Control, Environment, and Management (HNICEM). pp. 1–6 (2019). <https://doi.org/10.1109/HNICEM48295.2019.9072869>
2. Anguelov, D., Srinivasan, P., Koller, D., Thrun, S., Rodgers, J., Davis, J.: Scape: Shape completion and animation of people. *ACM Trans. Graph.* **24**(3), 408–416 (Jul 2005). <https://doi.org/10.1145/1073204.1073207>
3. Anthroscan: Human solutions gmbh. anthroscan. <https://www.human-solutions.com/> (2014), accessed: 2023-10-06
4. Armando, M., Boissieux, L., Boyer, E., Franco, J.S., Humenberger, M., Legras, C., Leroy, V., Marsot, M., Pansiot, J., Pujades, S., Rekik, R., Rogez, G., Swamy, A., Wuhrer, S.: 4dhumanoutfit: A multi-subject 4d dataset of human motion sequences in varying outfits exhibiting large displacements. *Computer Vision and Image Understanding* **237**, 103836 (Dec 2023). <https://doi.org/10.1016/j.cviu.2023.103836>
5. Bartol, K., Bojanić, D., Petković, T., Pribanić, T.: A review of body measurement using 3d scanning. *IEEE Access* **9**, 67281–67301 (2021). <https://doi.org/10.1109/ACCESS.2021.3076595>
6. Bogo, F., Romero, J., Pons-Moll, G., Black, M.J.: Dynamic FAUST: Registering human bodies in motion. In: *IEEE Conf. on Computer Vision and Pattern Recognition (CVPR)* (Jul 2017)
7. Bojanić, D., Bartol, K., Petković, T., Pribanić, T.: Direct 3d body measurement estimation from sparse landmarks. In: *Proceedings of the 19th International Joint Conference on Computer Vision, Imaging and Computer Graphics Theory and Applications - Volume 4: VISAPP*. pp. 524–531. INSTICC, SciTePress (2024). <https://doi.org/10.5220/0012384000003660>
8. Bojanić, D.: Smpl-fitting. <https://github.com/DavidBoja/SMPL-Fitting> (2024), accessed: 2024-08-20
9. Bougourd, J., Treleaven, P.: Uk national sizing survey–sizeuk. In: *International Conference on 3D Body Scanning Technologies*, Lugano, Switzerland. pp. 19–20 (2010). <https://doi.org/10.15221/10.327>
10. Casadei, K., Kiel, J.: *Anthropometric Measurement*. StatPearls Publishing, Treasure Island (FL) (2020), <http://europepmc.org/books/NBK537315>

11. Chang, C.C., Lin, C.J.: LIBSVM. *ACM Transactions on Intelligent Systems and Technology* **2**(3), 1–27 (Apr 2011). <https://doi.org/10.1145/1961189.1961199>
12. D. Camba, J., Leon, A., Cantero, J., Saorín, J., Contero, M.: Application of low-cost 3d scanning technologies to the development of educational augmented reality content. In: *FIE 2016*. pp. 1–6 (10 2016). <https://doi.org/10.1109/FIE.2016.7757673>
13. Dao, N.L., Deng, T., Cai, J.: Fast and automatic body circular measurement based on a single kinect. In: *Signal and Information Processing Association Annual Summit and Conference (APSIPA), 2014 Asia-Pacific*. pp. 1–4 (2014). <https://doi.org/10.1109/APSIPA.2014.7041571>
14. Deng, L., Yan, T., Zhao, Q.: Anthropometric parameter measurement from equivariant multi-view images. *Journal of Physics: Conference Series* **1576**(1), 012006 (jun 2020). <https://doi.org/10.1088/1742-6596/1576/1/012006>
15. Donlić, M.: Three-dimensional analysis of back surface under dynamic conditions in scoliosis diagnostics. Ph.D. thesis, Faculty of Electrical Engineering and Computing, University of Zagreb (2019)
16. de Ferreira, W.F., Balreira, D.G., Filho, D.M., Walter, M.: A template-based anthropometric measurement approach for 3d scanned bodies. In: *2023 36th SIBGRAPI Conference on Graphics, Patterns and Images (SIBGRAPI)*. IEEE (Nov 2023). <https://doi.org/10.1109/sibgrapi59091.2023.10347148>
17. Garcia-D’Urso, N.E., Azorin-Lopez, J., Fuster-Guillo, A.: A Template-Based Method for Automatic Anthropometric Measurements from Multiple 3D Scans, p. 157–168. Springer International Publishing (Nov 2022). https://doi.org/10.1007/978-3-031-21333-5_16
18. Geladi, P., Kowalski, B.R.: Partial least-squares regression: a tutorial. *Analytica Chimica Acta* **185**, 1–17 (1986). [https://doi.org/10.1016/0003-2670\(86\)80028-9](https://doi.org/10.1016/0003-2670(86)80028-9)
19. Giancola, S., Valenti, M., Sala, R.: A survey on 3d cameras: Metrological comparison of time-of-flight, structured-light and active stereoscopy technologies. In: *SpringerBriefs in Computer Science* (2018)
20. Gonzalez Tejeda, Y., Mayer, H.A.: Calvis: chest, waist and pelvis circumference from 3d human body meshes as ground truth for deep learning (2020)
21. Gordon, C., Churchill, T., Clauser, C., Bradtmiller, B., McConville, J., Tebbetts, L., Walker, R.: 1988 anthropometric survey of u.s. army personnel: Methods and summary statistics (01 1989)
22. Gordon, C.C., Churchill, T., Clauser, C.E., Bradtmiller, B., Mcconville, J.T.: Anthropometric survey of u.s. army personnel: Methods and summary statistics 1988 (1989), <https://api.semanticscholar.org/CorpusID:109169613>
23. Han, H.: Development of automatic 3d body scan measurement line generation method. *International Journal of Clothing Science and Technology* **35**(3), 350–362 (2023)
24. Hasler, N., Stoll, C., Sunkel, M., Rosenhahn, B., Seidel, H.P.: A Statistical Model of Human Pose and Body Shape. *Computer Graphics Forum* (2009). <https://doi.org/10.1111/j.1467-8659.2009.01373.x>
25. Heymsfield, S.B., Bourgeois, B., Ng, B.K., Sommer, M.J., Li, X., Shepherd, J.A.: Digital anthropometry: a critical review. *European journal of clinical nutrition* **72**(5), 680–687 (2018)
26. Hirshberg, D.A., Loper, M., Rachlin, E., Black, M.J.: Coregistration: Simultaneous alignment and modeling of articulated 3d shape. In: *Computer Vision – ECCV 2012*, pp. 242–255. Springer Berlin Heidelberg (2012). https://doi.org/10.1007/978-3-642-33783-3_18

27. Ionescu, C., Papava, D., Olaru, V., Sminchisescu, C.: Human3.6m: Large scale datasets and predictive methods for 3d human sensing in natural environments. *IEEE Transactions on Pattern Analysis and Machine Intelligence* **36**(7), 1325–1339 (jul 2014)
28. 3-D scanning methodologies for internationally compatible anthropometric databases - Part 1: Evaluation protocol for body dimensions extracted from 3-D body scans. Standard, International Organization for Standardization (2018)
29. Basic human body measurements for technological design - Part 1: Body measurement definitions and landmarks. Standard, International Organization for Standardization (2017)
30. Kaashki, N.N., Hu, P., Munteanu, A.: Deep learning-based automated extraction of anthropometric measurements from a single 3-d scan. *IEEE Transactions on Instrumentation and Measurement* **70**, 1–14 (2021). <https://doi.org/10.1109/tim.2021.3106126>
31. Kaashki, N.N., Hu, P., Munteanu, A.: Anet: A deep neural network for automatic 3d anthropometric measurement extraction. *IEEE Transactions on Multimedia* **25**, 831–844 (2023). <https://doi.org/10.1109/tmm.2021.3132487>
32. Kouchi, M., Mochimaru, M.: Errors in landmarking and the evaluation of the accuracy of traditional and 3d anthropometry. *Applied Ergonomics* **42**(3), 518–527 (Mar 2011). <https://doi.org/10.1016/j.apergo.2010.09.011>
33. Lassner, C., Romero, J., Kiefel, M., Bogo, F., Black, M.J., Gehler, P.V.: Unite the people: Closing the loop between 3d and 2d human representations. In: *IEEE Conf. on Computer Vision and Pattern Recognition (CVPR)* (Jul 2017), <http://up.is.tuebingen.mpg.de>
34. Li, P., Paquette, S.: Predicting anthropometric measurements from 3d body scans: Methods and evaluation. In: Di Nicolantonio, M., Rossi, E., Alexander, T. (eds.) *Advances in Additive Manufacturing, Modeling Systems and 3D Prototyping*. pp. 561–570. Springer International Publishing, Cham (2020)
35. Li, R., Yang, S., Ross, D.A., Kanazawa, A.: Learn to dance with aist++: Music conditioned 3d dance generation (2021)
36. Li, Z., Jia, W., Mao, Z.H., Li, J., Chen, H.C., Zuo, W., Wang, K., Sun, M.: Anthropometric body measurements based on multi-view stereo image reconstruction. In: *2013 35th Annual International Conference of the IEEE Engineering in Medicine and Biology Society (EMBC)*. IEEE (Jul 2013). <https://doi.org/10.1109/embc.2013.6609513>
37. Loper, M., Mahmood, N., Romero, J., Pons-Moll, G., Black, M.J.: SMPL: A skinned multi-person linear model. *ACM Trans. Graphics (Proc. SIGGRAPH Asia)* **34**(6), 248:1–248:16 (Oct 2015)
38. Lu, J., Wang, M.: Automated anthropometric data collection using 3d whole body scanners. *Expert Systems with Applications* **35**(1-2), 407–414 (Jul 2008). <https://doi.org/10.1016/j.eswa.2007.07.008>
39. Luo, S., Zhang, Q., Feng, J.: Automatic location and semantic labeling of landmarks on 3d human body models. *Computational Visual Media* **8**(4), 553–570 (May 2022). <https://doi.org/10.1007/s41095-021-0254-4>
40. Mahmood, N., Ghorbani, N., Troje, N.F., Pons-Moll, G., Black, M.J.: AMASS: Archive of motion capture as surface shapes. In: *International Conference on Computer Vision*. pp. 5442–5451 (Oct 2019)
41. von Marcard, T., Henschel, R., Black, M., Rosenhahn, B., Pons-Moll, G.: Recovering accurate 3d human pose in the wild using imus and a moving camera. In: *European Conference on Computer Vision (ECCV)* (sep 2018)

42. Markiewicz, L., Witkowski, M., Sitnik, R., Mielicka, E.: 3d anthropometric algorithms for the estimation of measurements required for specialized garment design. *Expert Systems with Applications* **85**, 366–385 (Nov 2017). <https://doi.org/10.1016/j.eswa.2017.04.052>
43. Paquette, S., Gordon, C.C., Bradtmiller, B.: Anthropometric survey (ansur) ii pilot study: Methods and summary statistics (2009), <https://api.semanticscholar.org/CorpusID:108187802>
44. Park, B.K.D., Jung, H., Ebert, S.M., Corner, B.D., Reed, M.P.: Efficient model-based anthropometry under clothing using low-cost depth sensors. *Sensors* **24**(5), 1350 (Feb 2024). <https://doi.org/10.3390/s24051350>
45. Pishchulin, L., Wuhrer, S., Helten, T., Theobalt, C., Schiele, B.: Building statistical shape spaces for 3d human modeling. *Pattern Recognition* **67**, 276–286 (2017)
46. Pons-Moll, G., Romero, J., Mahmood, N., Black, M.J.: Dyna: A model of dynamic human shape in motion. *ACM Transactions on Graphics, (Proc. SIGGRAPH)* **34**(4), 120:1–120:14 (Aug 2015)
47. Pons-Moll, G., Taylor, J., Shotton, J., Hertzmann, A., Fitzgibbon, A.: Metric regression forests for human pose estimation. pp. 4.1–4.11 (01 2013). <https://doi.org/10.5244/C.27.4>
48. Probst, T., Fossati, A., Salzmann, M., Gool, L.V.: Efficient model-free anthropometry from depth data. In: 2017 International Conference on 3D Vision (3DV). IEEE (Oct 2017). <https://doi.org/10.1109/3dv.2017.00062>
49. Robinette, K.M., Daanen, H., Paquet, E.: The caesar project: a 3-d surface anthropometry survey. In: Second International Conference on 3-D Digital Imaging and Modeling (Cat. No.PR00062). pp. 380–386 (1999). <https://doi.org/10.1109/IM.1999.805368>
50. Robinson, M., Parkinson, M.: Estimating anthropometry with microsoft kinect (2013), <https://api.semanticscholar.org/CorpusID:42868835>
51. Sengupta, A., Budvytis, I., Cipolla, R.: Synthetic training for accurate 3d human pose and shape estimation in the wild. In: British Machine Vision Conference (BMVC) (September 2020)
52. Shcherbina, K.K., Fogt, E.V., Golovin, M.A., Chernikova, M.V., Kuzicheva, A.D.: Automation of full-size wheelchair user body 3d-scan dimensional signs registration. *The International Archives of the Photogrammetry, Remote Sensing and Spatial Information Sciences* **XLIV-2/W1-2021**, 189–193 (Apr 2021). <https://doi.org/10.5194/isprs-archives-xxiv-2-w1-2021-189-2021>
53. Shotton, J., Fitzgibbon, A., Cook, M., Sharp, T., Finocchio, M., Moore, R., Kipman, A., Blake, A.: Real-time human pose recognition in parts from single depth images. In: CVPR 2011. pp. 1297–1304 (2011). <https://doi.org/10.1109/CVPR.2011.5995316>
54. Sims, R., Marshall, R., Gyi, D., Summerskill, S., Case, K.: Collection of anthropometry from older and physically impaired persons: Traditional methods versus tc2 3-d body scanner. *International Journal of Industrial Ergonomics* **42**(1), 65–72 (Jan 2012). <https://doi.org/10.1016/j.ergon.2011.10.002>
55. Škorvánková, D., Riečický, A., Madaras, M.: Automatic estimation of anthropometric human body measurements. In: Proceedings of the 17th International Joint Conference on Computer Vision, Imaging and Computer Graphics Theory and Applications. SCITEPRESS - Science and Technology Publications (2022). <https://doi.org/10.5220/0010878100003124>
56. Trujillo-Jiménez, M.A., Navarro, P., Pazos, B., Morales, L., Ramallo, V., Paschetta, C., Azevedo, S.D., Ruderman, A., Pérez, O., Delrieux, C., Gonzalez-José, R.:

- body2vec: 3d point cloud reconstruction for precise anthropometry with hand-held devices. *Journal of Imaging* **6**(9), 94 (Sep 2020). <https://doi.org/10.3390/jimaging6090094>
57. Tsoli, A., Loper, M., Black, M.J.: Model-based anthropometry: Predicting measurements from 3d human scans in multiple poses. In: *IEEE Winter Conference on Applications of Computer Vision*. IEEE (Mar 2014). <https://doi.org/10.1109/wacv.2014.6836115>
 58. Tsoli, A., Mahmood, N., Black, M.J.: Breathing life into shape: capturing, modeling and animating 3d human breathing. *ACM Trans. Graph.* **33**(4) (jul 2014). <https://doi.org/10.1145/2601097.2601225>
 59. Uriel, J., Ruescas, A., Iranzo, S., Ballester, A., Parrilla, E., Remón, A., Alemany, S.: A methodology to obtain anthropometric measurements from 4d scans. In: *Proceedings of the 7th International Digital Human Modeling Symposium - University of Iowa Libraries Publishing* (Aug 2022). <https://doi.org/10.17077/dhm.31758>
 60. Min-yang Wang, E., Wang, M.J., Yeh, W.Y., Shih, Y.C., Lin, Y.C.: Development of anthropometric work environment for taiwanese workers. *International Journal of Industrial Ergonomics* **23**(1–2), 3–8 (Jan 1999). [https://doi.org/10.1016/s0169-8141\(97\)00095-4](https://doi.org/10.1016/s0169-8141(97)00095-4)
 61. Wang, M.J.J., Wu, W.Y., Lin, K.C., Yang, S.N., Lu, J.M.: Automated anthropometric data collection from three-dimensional digital human models. *The International Journal of Advanced Manufacturing Technology* **32**(1-2), 109–115 (Feb 2006). <https://doi.org/10.1007/s00170-005-0307-3>
 62. Wang, Q., Jagadeesh, V., Ressler, B., Piramuthu, R.: Im2fit: Fast 3d model fitting and anthropometrics using single consumer depth camera and synthetic data. In: *3D Image Processing, Measurement , and Applications* (2014), <https://api.semanticscholar.org/CorpusID:13471>
 63. Wasenmuller, O., Peters, J.C., Golyanik, V., Stricker, D.: Precise and automatic anthropometric measurement extraction using template registration. In: *Proceedings of the 6th International Conference on 3D Body Scanning Technologies*, Lugano, Switzerland, 27-28 October 2015. Hometrica Consulting - Dr. Nicola D'Apuzzo (Oct 2015). <https://doi.org/10.15221/15.155>
 64. Weiss, A., Hirshberg, D., Black, M.J.: Home 3d body scans from noisy image and range data. In: *2011 International Conference on Computer Vision*. pp. 1951–1958 (2011). <https://doi.org/10.1109/ICCV.2011.6126465>
 65. Wuhrer, S., Azouz, Z.B., Shu, C.: Semi-automatic prediction of landmarks on human models in varying poses. In: *2010 Canadian Conference on Computer and Robot Vision*. pp. 136–142 (2010). <https://doi.org/10.1109/CRV.2010.25>
 66. Xiaohui, T., Xiaoyu, P., Liwen, L., Qing, X.: Automatic human body feature extraction and personal size measurement. *Journal of Visual Languages & Computing* **47**, 9–18 (Aug 2018). <https://doi.org/10.1016/j.jv1c.2018.05.002>
 67. Xie, H., Zhong, Y., Yu, Z., Hussain, A., Chen, G.: Automatic 3d human body landmarks extraction and measurement based on mean curvature skeleton for tailoring. *The Journal of The Textile Institute* **113**(8), 1677–1687 (Jul 2021). <https://doi.org/10.1080/00405000.2021.1944513>
 68. Yan, S., Wirta, J., Kämäräinen, J.K.: Anthropometric clothing measurements from 3d body scans. *Machine Vision and Applications* **31**(1-2) (Jan 2020). <https://doi.org/10.1007/s00138-019-01054-4>
 69. Yin, F., Zhou, S.: Accurate estimation of body height from a single depth image via a four-stage developing network. In: *2020 IEEE/CVF Conference on Computer Vision and Pattern Recognition (CVPR)*. pp. 8264–8273 (2020). <https://doi.org/10.1109/CVPR42600.2020.00829>

70. Zakaria, N., Gupta, D.: Anthropometry, Apparel Sizing and Design. The Textile Institute Book Series, Elsevier Science (2019), <https://books.google.hr/books?id=sOKODwAAQBAJ>
71. Zhong, Y., Li, D., Wu, G., Hu, P.: Automatic body measurement based on slicing loops. *International Journal of Clothing Science and Technology* **30**(3), 380–397 (Jun 2018). <https://doi.org/10.1108/ijcst-06-2017-0086>
72. Zou, H., Hastie, T.: Regularization and variable selection via the elastic net. *Journal of the Royal Statistical Society Series B: Statistical Methodology* **67**(2), 301–320 (Mar 2005). <https://doi.org/10.1111/j.1467-9868.2005.00503.x>
73. Škorvánková, D., Madaras, M.: Inception network for anthropometric body measurements estimation from structured point clouds. In: *Proceedings of the 10th International Conference on Software Development and Technologies for Enhancing Accessibility and Fighting Info-exclusion. DSAI 2022*, ACM (Aug 2022). <https://doi.org/10.1145/3563137.3563164>